ORGANIC PROCESS RESEARCH & DEVELOPMENT
OPR&D

pubs.acs.org/OPRD

Article

Direct Construction of Chiral Ether via Highly Efficient Heck Reaction and N-Directed Asymmetric Hydrogenation for Large-Scale Synthesis of MALT1 Inhibitor RGT-068A

Song Feng,* Haishen Zhang, Zhiyong Tang, Xingao Peng, Min Yang, Xudong Wei, and Wenge Zhong

Cite This: *Org. Process Res. Dev.* 2022, 26, 3089−3095

Read Online

ACCESS | Metrics & More | Article Recommendations | Supporting Information

ABSTRACT: Chemical process development e□orts leading to the large-scale production of RGT-068A are discussed. Process optimization resulted in (1) successful replacement of the Stille coupling reaction involving toxic stannane reagent via highly e□cient Heck reaction of methyl vinyl ether, (2) construction of the chiral ether unit through N-directed Ru-catalyzed asymmetric hydrogenation avoiding super-critical fluid chromatography (SFC) chiral separation, and (3) a streamlined process with a significantly improved overall yield of about 25%, 5-fold higher than the original discovery synthetic route, which enabled the delivery of high-quality material for IND-enabling studies.

KEYWORDS: *Heck reaction, vinyl ether, asymmetric hydrogenation, Stille coupling, urea*

INTRODUCTION

Mucosa-associated lymphoid tissue lymphoma translocation protein-1 (MALT1) is a key immunomodulator of the classical NF-κB signaling pathway, and it is involved in many diseases directly or indirectly.[1−5] Dysregulation of MALT1 activity contributes to the development of diseases such as MALT1-dependent inflammatory and/or autoimmune diseases such as rheumatoid arthritis (RA) and multiple sclerosis (MS). In recent years, emerging evidence also suggested that MALT1 plays an important role in the progression of systemic lupus erythematosus (SLE), primary Sjögren's syndrome (pSS), and cancer such as B-cell lymphoma. Thus, modulating MALT1 function is considered a potentially viable approach that can have direct and indirect benefits in a variety of inflammatory disorders and cancers.[6−8]

For an ongoing research and development program at Regor, we have discovered the pyrazoloaminopyrimidine compound RGT-068A (1), a highly potent MALT1 inhibitor with good oral bioavailability (Figure 1). It was selected as a promising preclinical candidate for further development to potentially treat autoimmune diseases with significant unmet medical needs. To support the whole suite of IND-enabling studies, process chemistry development and delivery of drug substance at kilogram scale were needed. While the discovery synthesis of RGT-068A was straightforward in terms of bond construction strategy, there was significant room for reaction condition improvement to ensure a suitable process for the large-scale production of the drug substance. Herein, we report our e□orts that resulted in a practical and highly e□cient synthesis of RGT-068A.

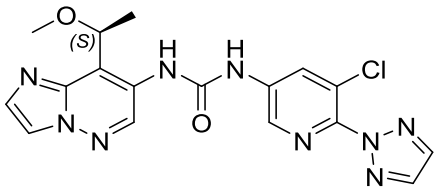

RGT-068A (**1**)

Figure 1. RGT-068A (**1**), a potent and selective MALT1 inhibitor.

RESULTS AND DISCUSSION

Discovery Synthetic Route to RGT-068A (1). As shown in Scheme 1, the discovery synthesis of **1** started with the saponification of ester **2** to give acid **3** in a 90% yield. Curtius rearrangement in the presence of diphenyl phosphoryl azide (DPPA) and concurrent treatment with Boc_2O a□orded Boc-protected amine intermediate **4** in a 58% yield. Subsequent Stille coupling of intermediate **4** with organo-stannane compound **5i** produced vinyl ether intermediate **5** in a 70% yield, which was converted to ketone **6** upon treatment with aqueous HCl in around 80% yield. After reduction with sodium borohydride ($NaBH_4$), the resulting secondary alcohol **7** was reacted with thionyl chloride ($SOCl_2$), followed by quenching with methanol, to provide the corresponding ether **8** in 50−60% yields (three transformations). The completion of the synthesis of **1** involved urea formation of amine **8** with active carbamate (**9i**) using Et_3N as a base to furnish the racemic urea compound **9** in a 70% yield after silica gel chromatography. A final chiral separation by super-critical fluid

Received: July 21, 2022
Published: November 3, 2022

https://doi.org/10.1021/acs.oprd.2c00229
Org. Process Res. Dev. 2022, 26, 3089−3095

Scheme 1. Synthesis of 1 via the Discovery Route[a]

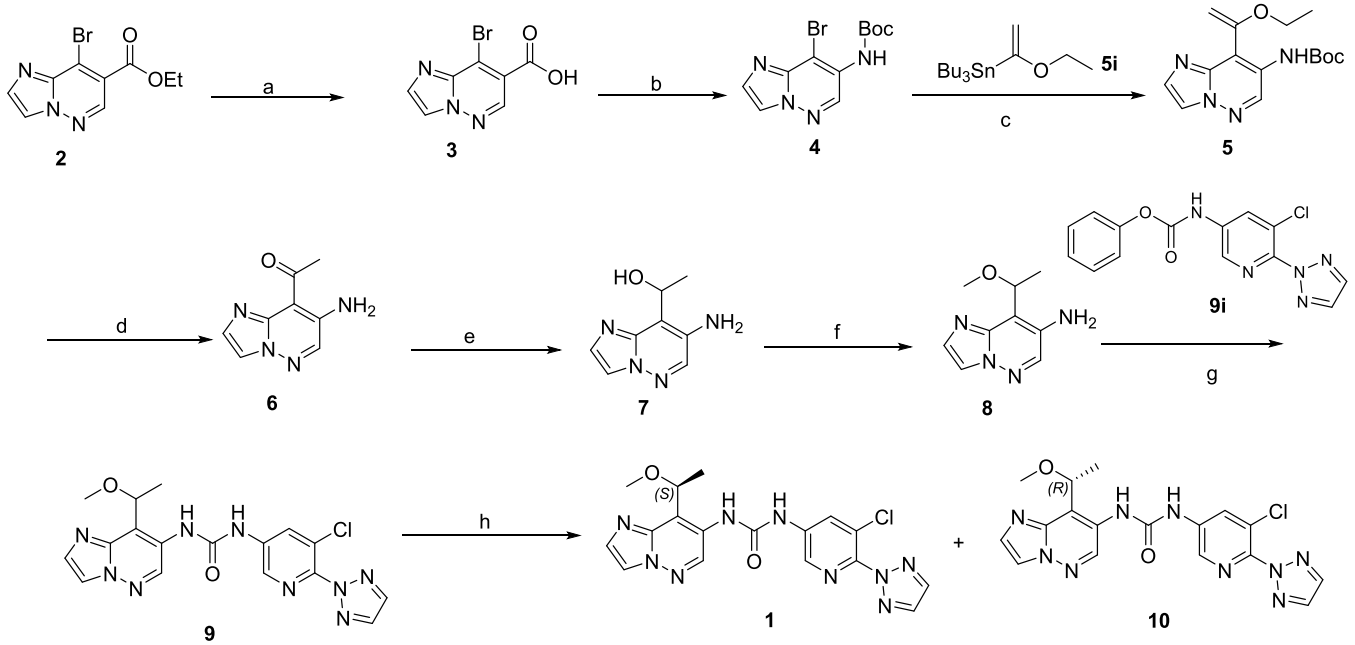

[a]Reagents and conditions: (a) LiOH, THF, EtOH, 0–10 °C, 30 min, 90%; (b) DPPA, TEA, Boc_2O, *t*-BuOH, toluene, 80 °C, 3 h, 58%; (c) **5i**, $Pd(dppf)Cl_2CH_2Cl_2$, DMF, *t*-BuOH, 90 °C, 66 h, 70%; (d) 6 N HCl, dioxane, 80%; (e) $NaBH_4$, MeOH, 2 h, 70–80%; (f) $SOCl_2$, MeOH, 3 h, 80%; (g) **9i**, Et_3N, 50%; and (h) SFC chiral separation, 45%.

Scheme 2. Exploratory Experiments for the New Synthetic Route[a]

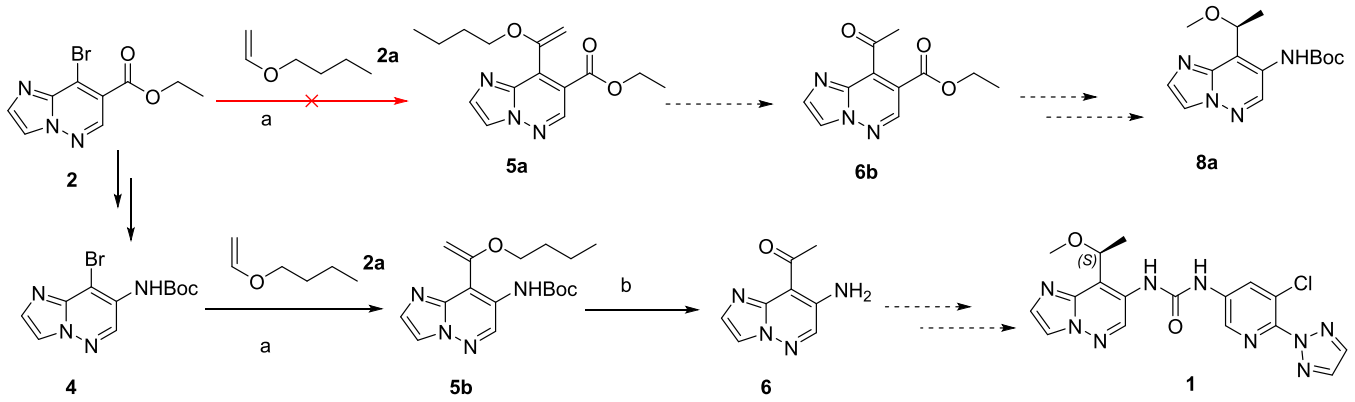

[a]Reagents and conditions: (a) **2a** (8.0 equiv), $Pd(dppf)Cl_2CH_2Cl_2$, *n*-BuOH, $NaHCO_3$, LiOTf, 16 h, 83% and (b) 6 N HCl, 3 h, 58%.

chromatography (SFC) eventually afforded the desired single enantiomer RGT-068AA (**1**) in a 45% yield.

Overall, there were a total of eight linear steps from the raw starting material **2** to the final enantiomer RGT-068A (**1**) including the last SFC chiral separation step, and the total yield was only about 5.0%. This discovery route was amenable to provide the gram-scale preparation of RGT-068A for early tox and PK/PD studies. However, it had two major areas for improvement, namely, the Stille coupling involving the highly toxic[9] and moisture-sensitive vinyl stannane reagent **5i** and the atomically noneconomical chiral separation step, which greatly limited the practical application of this route for large-scale GLP or GMP production and was not beneficial for environmental protection. Therefore, we decided to embark on chemistry efforts to investigate alternative synthetic strategies to overcome these challenges and to improve the overall manufacturing yield of RGT-068A.

General Strategy for Large-Scale Synthesis of RGT-068A. To circumvent the usage of toxic vinyl stannane reagent in the Stille coupling, direct Heck reaction with vinyl *n*-butyl ether was initially proposed to introduce the vinyl ether at the 8-position of imidazo[1,2-*b*]pyridazine (**2**) (Scheme 2). Such Heck reaction with vinyl *n*-butyl ether has been successfully applied to the commercial manufacturing of Palbociclib.[10,11] However, for reasons not fully understood, our attempt to prepare **6b** by this method starting with **2** failed to provide any meaningful results. Contrary to this observation, with the Boc-protected amine intermediate **4**, the Heck reaction went smoothly and afforded the desired product **5b** in an 83% yield under the optimized conditions using $Pd(dppf)Cl_2CH_2Cl_2$ as the catalyst. As shown in Scheme 2, subsequent transformations of ketone formation, protection, reduction, and direct methylation followed by deprotection in steps b, c, d, etc., did not show significant improvement over either reaction

https://doi.org/10.1021/acs.oprd.2c00229
Org. Process Res. Dev. 2022, 26, 3089−3095

Scheme 3. Retrosynthetic Analysis of RGT-068A (1)

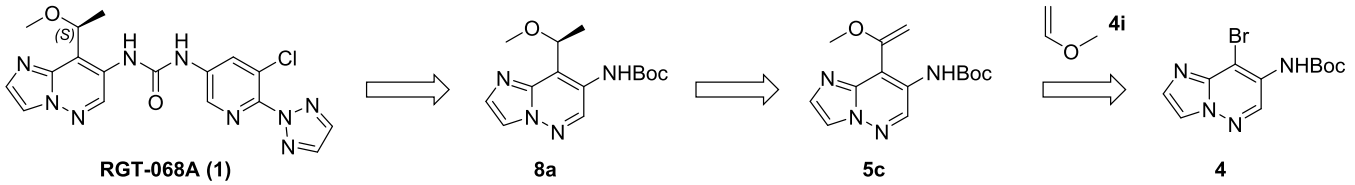

Table 1. Optimization of Conditions for the Heck Reaction of 4 with MVE 4i[a]

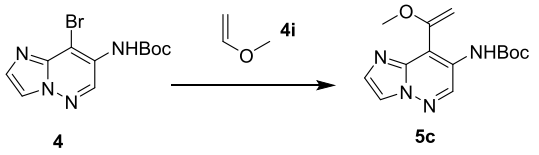

					conversion results[b]	
entry	base (3.0 equiv)	catalyst/ligands (0.2 equiv)	additive (1.0 equiv)	solvent	**4** (3.18 min)	**5c** (2.78 min)
1	$NaHCO_3$	$Pd(dppf)Cl_2CH_2Cl_2$	LiOTf	*n*-BuOH	66.3%	8.5%
2	K_3PO_4	$Pd(dppf)Cl_2CH_2Cl_2$	LiOTf	n-BuOH	23.1%	9.3%
3	Na_2CO_3	$Pd(dppf)Cl_2CH_2Cl_2$	LiOTf	*n*-BuOH	23.4%	43.5%
4	Na_2CO_3	$Pd(dtbpf)Cl_2$	LiOTf	*n*-BuOH	64%	N.D.
5	Na_2CO_3	$Pd(OAc)_2$/DPPP	LiOTf	*n*-BuOH	56%	0.8%
6	Na_2CO_3	$Pd(dppf)Cl_2CH_2Cl_2$	LiOTf	EtOH	53.7%	21.7%
7	Na_2CO_3	$Pd(dppf)Cl_2CH_2Cl_2$	LiOTf	DMSO	37%	9.0%
8	Na_2CO_3	$Pd(dppf)Cl_2CH_2Cl_2$	LiOTf	TAA	0.8%	72.8%
10	Na_2CO_3	$Pd(dppf)Cl_2CH_2Cl_2$	LiOTf	*t*-BuOH	0.5%	82.7%

[a]**4** (1.0 g, 1.0 equiv), MVE **4i** (1.5 g, 8.0 equiv), 87 h, 90 °C. [b]Checked by HPLC.

yield or chiral center construction; new alternative synthetic methods were still warranted.

Encouraged by the promising Heck reaction results, we contemplated if it is feasible to establish the desired stereochemistry of RGT-068A by direct asymmetric hydrogenation of the Heck reaction vinyl ether product. As shown in the retrosynthetic analysis (Scheme 3), we envisioned that key intermediate **8a** with the desired chirality could potentially be obtained by the direct asymmetric hydrogenation of the other key methyl vinyl ether intermediate **5c**, while **5c**, in turn, could be produced under modified Heck reaction conditions established above. In the following, we detail our efforts in optimizing these reactions and developing the process chemistry for the large-scale synthesis of RGT-068A for IND-enabling studies.

Heck Reaction of Bromo-imidazopyridazine 4 with Methyl Vinyl Ether 4i (MVE). Given that the Heck reaction of intermediate **4** with *n*-butyl vinyl ether was successful, we believed that it should also be applicable to obtain intermediate **5c** using methyl vinyl ether. Indeed, the initial results were promising. It was worth noting that due to the relatively low boiling point and volatility of methyl vinyl ether (MVE, **4i**), the Heck coupling reaction had to be carried out in a pressure vessel, while the molar equivalence of the MVE was greatly excessive. Since MVE could be easily removed during workup, the scale-up of this step was considered quite convenient. To optimize Heck reaction conditions and improve reaction yields, we further screened bases, catalysts, and solvents and the selected results are summarized in Table 1.

As entry 1 in Table 1 indicated, the condition using $NaHCO_3$ as the base that worked well for the synthesis of **5b** did not give satisfactory results. While K_3PO_4 showed no improvement over $NaHCO_3$, the use of Na_2CO_3 significantly increased the yield of **5c** formation. A quick catalyst survey of commonly used catalysts for Heck reactions revealed that $Pd(dppf)Cl_2CH_2Cl_2$ provided the best results (entries 4 and 5; please switch entries 7 and 8 to become new entries 4 and 5). We next screened solvents and found that EtOH and DMSO were not effective solvents; conversion rates below 30% were observed (entries 6 and 7). Eventually, we found that *tert*-amyl alcohol(TAA) and *t*-BuOH are the two most suitable solvents, providing **5c** conversion of 72.8 and 82.7%, respectively. For all subsequent scale-up and process work, we selected the optimal condition of using *t*-buOH as the solvent, $Pd(DPPF)Cl_2CH_2Cl_2$ as the catalyst, Na_2CO_3 as the base, and LiOTf as an additive, which was able to boost good yield and selectivity, as reported.[12]

Ru-Catalyzed Asymmetric Hydrogenation of 5c. Next, we investigated the direct asymmetric hydrogenation of viny ether **5c** with several commercially available ruthenium catalysts. Rhodium- and ruthenium-catalyzed asymmetric hydrogenation of functionalized vinyl compounds have been recognized as one of the most useful reactions for the preparation of optically active compounds, especially for vinyl substrates that bear a neighboring coordinating functional group such as amide and ester.[10,13] We recently reported a highly efficient and stereoselective Ru-catalyzed asymmetric hydrogenation of vinyl ethers without such functional groups but instead with potential neighboring N-atom participation.[14] We adapted the condition for **5c** and pleasantly found that the asymmetric hydrogenation on the α-substituted imidazolepyridazine vinyl ether proceeded smoothly with RuCl(*p*-cymene)-((*S*)-BINAP) or (*R*)-Ru(OAC)$_2$(BINAP) as the catalyst, resulting in good conversion and promising enantioselectivity (entries 3 and 4, Table 2).

https://doi.org/10.1021/acs.oprd.2c00229
Org. Process Res. Dev. 2022, 26, 3089−3095

Table 2. Ru-Catalyst Screening Results for the Asymmetric Hydrogenation of 5c[a]

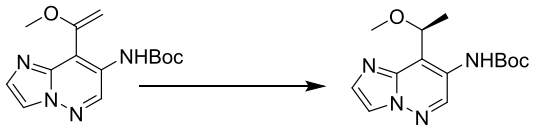

5c **8a**

entry	catalyst (0.02 equiv)	IPC percentage (%)[b]	ee (%)[c]
1	RuCl[(S)-xylbinap][(S,S)-dpen]	**5c** (2.76min):56.2 **8a** (3.0min):24.3	22.8
2	(S)-RuCl[(*p*-cymene)(DM-BINAP)]Cl	**5c** (2.78 min):32.6 **8a** (3.0min):43.5	28.4
3	$Ru(OAc)_2$[(S)-binap]	**5c**(2.82min):0.6 **8a**(2.91min):84.4	46.6
4	(S)-RuCl[(*p*-cymene)(binap)Cl]	**5c** (2.76min):0.1 **8a** (3.0min):72.3	55.4

[a]**5c** (29 mg,1.0 equiv)EtOH (1 mL, 33.0 V), RT. [b]In process control (IPC). [c]Checked by chiral HPLC.

To further improve enantioselectivity, various solvents were screened with (*S*)-RuCl[(*p*-cymene)(binap)Cl] as the catalyst of choice. The results are summarized in Table 3. Similar to the effects of solvents reported in the literature,[15,16] the asymmetric hydrogenation of vinyl ether substituted with heteroaryl catalyzed by Ru-BINAP proceeded well with high conversion rate in either methanol, ethanol, or iso-propanol (IPA). However, the enantioselectivity in IPA was apparently better than in either methanol or ethanol (entries 1–3). Consistent with the trend, less polar solvents gave better results on enantioselectivity. While ethyl acetate (EA), THF, and $PhCH_3$ all demonstrated improved ee values over IPA (entries 4–6), DCM yielded the best enantioselectivity among solvents we screened (entry 7, ee 93%). After further optimization of reaction conditions with DCM as solvent and crystallization investigation, the chiral purity of 97% ee for product **8a** was achieved.

Table 3. Reaction Solvent Screening Results of the Asymmetric Hydrogenation of 5c

entry	solvent (2 mL)	IPC percentage (%)[a]	ee (%)[b]
1	MeOH	**5c**: N.D. **8a**:88.5	35.0
2	EtOH	**5c**: 0.1 **8a**: 72.3	55.4
3	IPA	**5c**: N.D. **8a**: 89.3	78.0
4	EA	**5c**: 24.0 **8a**: 52.0	83.0
5	THF	**5c**: N.D. **8a**: 83.7	87.0
6	PhMe	**5c**: N.D. **8a**: 91.9	89.2
7	DCM	**5c**: 0.2 **8a**: 90	93.6

[a]**5c** (60 mg,1.0 equiv) (*S*)-RuCl[(*p*-cymene)(binap)Cl](3.7 mg, 0.02 equiv) RT; *b* H_2 5 Mpa, RT, RuCl(*p*-cymene)((*S*)-BINAP). In process control (IPC). [b]Checked by chiral HPLC.

Urea Formation Leading to the Synthesis of RGT-068A (1). After successfully establishing the tandem Heck and Ru-catalyzed asymmetric hydrogenation reactions, we turned our attention to the final chemical bond construction step of urea formation to complete the synthesis of RGT-068A (Scheme 4). The urea functionality is present in many drug molecules.[17] For this reason, a variety of synthetic methodologies for the preparation of urea derivatives have been developed.[18−20] Curtius, Lossen, and Hofmann rearrangements are also employed to generate urea derivatives through the isocyanate intermediates. Unlike other urea formation reactions, the weak basicity of the imidazolepyridazine amine **11** renders it difficult to harness the urea-forming approaches mentioned above (yields < 40%). The initial strategy in the medicinal chemistry route to address the issues was to exploit carbamate derivatives, the precursor of urea, to perform aminolysis with weakly basic amine **11** under alkaline conditions. Multiple solvents were evaluated and screened, as revealed in Table 4; THF and DCM turned out to be the best solvents with conversion rates of 47.4 and 49.6%, respectively. More in-depth studies suggested that the low yields of the reactions were mainly due to the relatively poor stability of carbamate (**9i**). To mitigate this problem, new amine intermediate **11i** was employed for the preparation of urea **1** and the reaction conditions were optimized.

Scheme 4. Urea Formation to Generate 1[a,b]

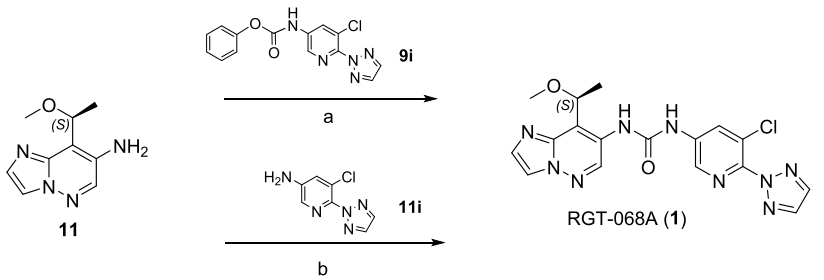

[a]**11** (1.0 equiv) **9i** (1.2 equiv) 50 °C, **THF**(5 mL, 10.0 V). [b](1) Bis(trichloromethyl)carbonate (**BTC**) (0.5 equiv), **11i** (1.0 equiv), (2) DCM (20 mL, 20V), Et_3N (1.0 equiv), 1 h at 0–10 °C.

https://doi.org/10.1021/acs.oprd.2c00229
Org. Process Res. Dev. 2022, 26, 3089−3095

Table 4. Optimization of Urea Formation

		IPC percentage (220 nm)[a]		
entry	solvent	**11** (RT: 0.73 min)[b]	**11i** (RT: 3.63 min)[b]	**1** (RT: 2.68 min)[b]
1	DMF	2.0	1.6	40.8
2	DMSO	4.9	0.1	46.1
3	THF	5.7	8.2	47.7
4	dioxane	9.6	36.9	24.4
5	ACN	29.4	7.9	2.7
6	DCM	4.3	6.2	49.7
7	ACN	5.0	7.2	73.8[c]

[a](1) Bis(trichloromethyl)carbonate (**BTC**) (0.5 equiv), **9i** (1.0 equiv), (2) DCM (20 mL, 20 V), Et_3N (1.0 equiv), 1 h at 0−10 °C; several other small peaks were not identified due to their signals are very weak. In process control (IPC), checked by HPLC. [b]HPLC RT: retention time. [c]Several other conditions like water contents, material charging order, etc., are optimal.

The BTC itself is relatively more active; treatment with intermediate amine **11** or **11i** can furnish the corresponding active isocyanates, which, in turn, can react with another amine to afford urea derivatives. To better control the potential symmetrical urea impurities, the reaction was divided into two stages; in each stage, the amount of BTC, reaction solvent, and base were further optimized. The content of water in the reaction system also has a remarkable impact on the conversion rate; in the presence of an activated molecular sieve, the yield of the urea formation step can increase from 62.5 to 73.8%. Eventually, the optimal reaction conditions for urea formation were determined and successfully applied to the kilogram scale-up production of RGT-068A (**1**).

Scaled-Up Synthesis of RGT-068A (1). Scheme 5 outlines the consistent and reproducible process for the large-scale synthesis of RGT-068A (**1**) with high chemical purity (99.4%) and high enantiomeric purity (97.1% ee). The synthesis of the key intermediates 4 and 2 can be referred to in some literature. Some limitations for the urea formation step were observed and worthy of further optimization in the future. The final experimental details are described in the Experimental Section. Compared to the initial medicinal chemistry, small-scale synthetic route involving eight steps with a 5% overall yield, the new methods described above that were used for the kilogram-scale synthesis of RGT-068A (**1**) are highly effective and in excellent overall yield (six steps, ~25%); more than 500 g of RGT-068A scale-up has been conducted and delivered, which ensured the adequate supply of drug substance for IND-enabling preclinical studies.

EXPERIMENTAL SECTION

General. Unless otherwise noted, all of the reagents and solvents were purchased from commercial suppliers and used without further purification. All of the reactions were carried out under nitrogen. ^1H and ^{13}C NMR spectra were recorded on Bruker ADVANCE III HD (300 MHz)/BRUKER AVANCE NEO (400 MHZ) spectrometers. $CDCl_3$/DMSO-d_6 was the solvent used for the NMR analysis, with tetramethylsilane as the internal standard. Chemical shifts were reported upfield to TMS (0.00 ppm) for ^1H NMR and relative to $CDCl_3$ (77.0 ppm) for ^{13}C NMR. Chemical shifts are reported in parts per million relative to the residual deuterated DMSO for ^1H and ^{13}C, and J values are expressed in hertz. New products were further characterized by HRMS. HPLC analysis was performed on an Agilent 1260 instrument. LC-MS analysis was performed on an Agilent 1260 HPLC + G 6125 MS instrument. Column chromatography was performed with silica gel (Rushanshi Shuangbang Xincailiao Co., Ltd.). All yields are uncorrected for purity. The following abbreviations are used to indicate multiplicities: s = singlet; d = doublet; t = triplet; q = quartet; m = multiplet.

*Synthesis of tert-Butyl (8-(1-Methoxyvinyl)imidazo[1,2-b]pyridazin-7-yl)carbamate (**5c**).* **4** (310 g, 1.0 equiv), Na_2CO_3 (315.5 g, 3.0 equiv), LiOTf (154.8 g, 1.0 equiv), Pd(dppf)$Cl_2CH_2Cl_2$ (40.51 g, 0.05 equiv), *t*-BuOH (1860 mL, 6.0 V), and MVE (**4i**, 461.1 g, 8.0 equiv) were added successively into a 5 L reactor; the reactor was sealed and stirred at 90 ± 5 °C for >24 h. After 50 h, the reaction mixture was periodically monitored by LC-MS until the complete consumption of starting material **4**. After cooling to rt, the suspension was filtered, and the pad was rinsed with EA at a 50 °C water bath; the filtrate was collected, concentrated in vacuo, and the crude solid product was further purified by short silica gel column chromatography with EA: PE = 1:3 as the mobile

Scheme 5. Scale-Up Route of RGT-068A (1)[a]

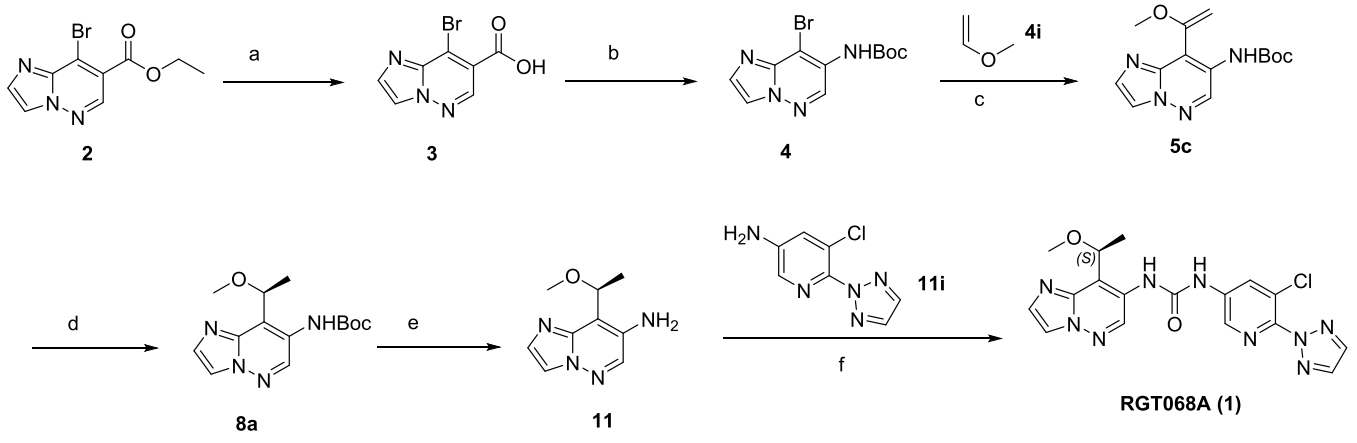

[a]Reagents and conditions: (a) LiOH, THF, EtOH, 0−10 °C, 30 min, 92%; (b) DPPA, TEA, Boc_2O, *t*-BuOH, toluene, 80 °C, 3 h, 59%; (c) methyl vinyl ether(MVE, **4i**) (8.0 equiv), Pd(dppf)$Cl_2CH_2Cl_2$, LiOTf/Na_2CO_3, *t*-BuOH, 90 °C, 66 h, 65%; (d) (*R*)-RuCl(*p*-cymene)(binap)Cl, DCM, H_2, 5 MPa, RT, 41 h, 93%; (e) TFA, DCM, 0−10 °C, 2 h, 87%; and (f) **11i**, BTC, Et_3N, 0−10 °C, 3 h, 75%.

https://doi.org/10.1021/acs.oprd.2c00229
Org. Process Res. Dev. 2022, 26, 3089−3095

phase to give the crude product (**5c**, 186 g, yield 64.8%) as a yellow solid. LC-MS(ESI) m/z: 291.2 [M + 1] ^{1}H NMR (400 MHz, $CDCl_3$-d_1), 8.78 (s, 1H), 7.86(s, 1H), 7.70 (d, J = 1.2 Hz, 1H), 7.69 (d, J = 1.6 Hz, 1H), 5.32 (d, J = 2.1 Hz, 1H), 4.92 (d, J = 2.4 Hz, 1H), 3.34 (s, 3H), 1.47 (s, 9H). ^{13}C NMR (101 MHz, DMSO-d_6) δ 153.22, 151.98, 142.48, 137.47, 133.66, 126.05, 117.04, 94.01, 80.59, 63.65, 28.41.

*Synthesis of tert-Butyl (S)-(8-(1-Methoxyethyl)imidazo-[1,2-b]pyridazin-7-yl)carbamate (**8a**).* DCM (897 mL,10.0 V), **5c** (89.7 g,1.0 equiv), and (R)-RuCl[(*p*-cymene)(binap)-Cl] (2.87 g, 0.01 equiv) were successively added to a 2 L reactor equipped with a mechanical stirrer. The flask was degassed and refilled with hydrogen three times; then, the hydrogen pressure was adjusted to 5 MPa. The reaction mixture was stirred at rt under a 5 MPa hydrogen pressure. After 20−30 h, till all of the starting material **5c** was completely consumed, the reaction mixture was filtered and the filtrate was concentrated to a□ord the crude product as an o□-white solid (**8a**, 82.5 g, yield 93%), which was directly used in the next step without further purification.

LC-MS(ESI) m/z: 293.2 [M + 1] ^{1}H NMR(400 MHz, $CDCl_3$-d_1) δ 8.85 (s, 1H), 8.66 (s, 1H), 8.15 (d, J = 4 Hz, 1H), 7.64 (d, J = 4 Hz, 1H), 5.17 (q, J = 8 Hz, 1H), 3.23 (s, 3H), 1.53 (d, 3H), 1.47 (s, 9H). ^{13}C NMR (101 MHz, DMSO-d_6) δ 153.01, 140.65, 138.00, 133.56, 126.40, 116.71, 81.10, 72.40, 64.90, 28.37, 20.15.

*Synthesis of RGT-068A (**1**).* ACN (850 mL, 10 V) and BTC (64.8 g, 0.5 equiv) were added to a 5 L three-necked bottle equipped with a mechanical stirrer; the reaction mixture was stirred at rt. To the reaction mixture, a solution of **11i** (85.0 g, 1.0 equiv) in ACN (1.7 L, 20 V) and Et_3N (44 g, 1.0 equiv) cooled in an ice−water bath was added dropwise. After addition, the resulting mixture was allowed to stir for 30 min, and additional 50 min, the reaction sample was checked by LC-MS till more than 95% starting material has been consumed. Nitrogen was bubbled into the reaction bottle to remove BTC for more than 1 h. To the reaction bottle, the mixture solution of 12 (76 g, 0.9 equiv), ACN (1.7 L, 20 V), and Et_3N (44 g, 1.0 equiv) was added and stirred for more than 15 h till the reaction went to completion. The pH value of the mixture was adjusted to around 3 with 6 N HCl, and the HCl salt of RGT-068A was obtained through filtration. DMSO (3.0 V) in a reaction bottle was stirred and heated at 80 °C; the HCl salt of RGT-068A was added in batches to the solution, the internal temperature was controlled at 80 ± 5 °C and stirred for at least 30 min, and then allowed to cool to rt and filtered; the pad was washed with ACN, and RGT-068A was obtained. The mixture of RGT-068A HCl salt and water (6.0 V) in a reaction bottle was stirred at rt, TEA was added, and the subsequent mixture was stirred for an additional 30 min till the pH was 8−9, filtrated, and the crude product RGT-068A (**1**) was obtained as an o□-white solid (290 g, 96.7%) with good purity and ee value (98.8 and 99.1%, respectively). LC-MS: m/z 414 $[M + H]^+$, ^{1}H NMR (DMSO-d_6, 400 MHz): δ 10.60 (s, 1H), 9.12 (s, 1H), 8.81 (s, 1H), 8.55 (d, J = 2.4 Hz, 1H), 8.50 (d, J = 2.4 Hz, 1H), 8.20 (d, J = 1.6 Hz, 1H), 8.16 (s, 2H), 7.67 (d, J = 1.2 Hz, 1H), 5.33 (q, J = 6.8 Hz, 1H), 3.34 (s, 3H), 1.56 (d, J = 6.4 Hz, 3H). ^{13}C NMR (101 MHz, DMSO-d_6) δ 152.64, 142.12, 141.21, 139.18, 138.38, 137.38, 136.61, 133.55, 127.99, 126.66, 126.49, 124.30, 116.84, 73.98, 57.27, 40.58, 40.37, 40.17, 39.96, 39.75, 39.54, 39.33, 19.51. HRMS (ESI) calcd for $C_{17}H_{16}ClN_9O_2$ $(M + H)^+$ 413.1115, found 413.1134.

ASSOCIATED CONTENT

Supporting Information

The Supporting Information is available free of charge at https://pubs.acs.org/doi/10.1021/acs.oprd.2c00229.

Synthesis of **3** and **4**, ^{1}H and ^{13}C NMR spectra of compounds **RGT-068A**, **5c**, **8a**, **11**, **2**, and **3**; and chiral HPLC spectra of **8a** (PDF)

AUTHOR INFORMATION

Corresponding Author

Song Feng − *Regor Therapeutics Group, Shanghai 201203, China;* orcid.org/0000-0001-7007-7765; Email: songfls@126.com

Authors

Haishen Zhang − *Pharmaron (Ningbo) Technology Development Co., Ningbo 315366 Zhejiang, China*

Zhiyong Tang − *Pharmaron (Ningbo) Technology Development Co., Ningbo 315366 Zhejiang, China*

Xingao Peng − *BioDuro-Sundia, Shanghai 201203, China*

Min Yang − *Regor Therapeutics Group, Shanghai 201203, China*

Xudong Wei − *Pharmaron (Ningbo) Technology Development Co., Ningbo 315366 Zhejiang, China*

Wenge Zhong − *Regor Therapeutics Group, Shanghai 201203, China*

Complete contact information is available at: https://pubs.acs.org/10.1021/acs.oprd.2c00229

Author Contributions

The manuscript was written through contributions of all authors. All authors have given approval to the final version of the manuscript.

Notes

The authors declare no competing financial interest.

ACKNOWLEDGMENTS

The authors thank Regor Therapeutics colleagues Drs Xiayang Qiu, Min Zhong, Xiaotian Zhu, Min Yang, and Xi Chen, and Yanny Nie for their great support of this work.

REFERENCES

(1) Yu, J. W.; Jeffrey, P. D.; Ha, J. Y.; Yang, X.; Shi, Y. Crystal structure of the mucosa-associated lymphoid tissue lymphoma translocation 1 (MALT1) paracaspase region. *Proc. Natl. Acad. Sci. U.S.A.* **2011**, *108*, 21004−21009.

(2) Jaworski, M.; Thome, M. The paracaspase MALT1: biological function and potential for therapeutic inhibition. *Cell. Mol. Life Sci.* **2016**, *73*, 459−473.

(3) Lee, C. H.; Bae, S. J.; Kim, M. Mucosa-associated lymphoid tissue lymphoma translocation 1 as a novel therapeutic target for rheumatoid arthritis. *Sci. Rep.* **2017**, *7*, No. 11889.

(4) Schlauderer, F.; Seeholzer, T.; Desfosses, A.; Gehring, T.; Strauss, M.; Hopfner, K. P.; Gutsche, I.; Krappmann, D.; Lammens, K. Molecular architecture and regulation of BCL10-MALT1 filaments. *Nat. Commun.* **2018**, *9*, No. 4041.

(5) Cheng, L.; Deng, N.; Yang, N.; Zhao, X.; Lin, X. Malt1 Protease Is Critical in Maintaining Function of Regulatory T Cells and May Be a Therapeutic Target for Antitumor Immunity. *J. Immunol.* **2019**, *202*, 3008−3019.

(6) Seshadri, M. R.; Melnick, A. M. Targeting MALT1 for the treatment of diffuse large B-cell lymphoma. *Leuk. Lymphoma* **2022**, *63*, 789−798.

(7) Liang, X. W.; Cao, Y. C.; Li, C. P.; Yu, H. L.; Yang, C. H.; Liu, H. MALT1 as a promising target to treat lymphoma and other diseases related to MALT1 anomalies. *Med. Res. Rev.* **2021**, *41*, 2388−2422.
(8) Solsona, B. G.; Schmitt, A.; Schulze-Osthoff, K.; Hailfinger, S. The Paracaspase MALT1 in Cancer. *Biomedicines* **2022**, *10*, No. 344.
(9) Lu, G.-P.; Cai, C.; Lipshutz, B. H. Stille couplings in water at room temperature. *Green Chem.* **2013**, *15*, 105−109.
(10) Burk, M. J. C2-symmetric bis(phospholanes) and their use in highly enantioselective hydrogenation reactions. *J. Am. Chem. Soc.* **1991**, *113*, 8518−8519.
(11) Li, T.; Su, M.; Zhang, Q.; Liu, Z.; Hu, X. Low-cost preparation of palbociclib. CN113683612.2021.
(12) Becica, J.; Glaze, O. D.; Hruszkewycz, D. P.; Dobereiner, G. E.; Leitch, D. C. The influence of additives on orthogonal reaction pathways in the Mizoroki−Heck arylation of vinyl ethers. *React. Chem. Eng.* **2021**, *6*, 1212−1219.
(13) Zhu, Y.; Burgess, K. Iridium catalyzed enantioselective hydrogenation of α-alkoxy and β-alkoxy vinyl ethers. *RSC Adv.* **2012**, *2*, 4728−4735.
(14) Feng, S.; Ren, B.; Li, L.; Xia, F.; Tang, Z.; Zhang, Y.; Liu, X.; Lu, Q.; Zhong, W. Highly efficient ruthenium-catalyzed asymmetric hydrogenation of N-heteroaryl vinyl ethers. *Org. Chem. Front.* **2022**, *9*, 3022−3026.
(15) Geng, C.; Zhu, R.; Zhang, D.; Lu, T.; Wheeler, S. E.; Liu, C. Solvent dependence of the stereoselectivity in bipyridine N,N′-dioxide catalyzed allylation of aromatic aldehydes: A computational perspective. *Mol. Catal.* **2020**, *483*, No. 110712.
(16) Wolfson, A.; Vankelecom, I. F. J.; Geresh, S.; Jacobs, P. A. The role of the solvent in the asymmetric hydrogenation of β-keto esters with Ru-BINAP. *J. Mol. Catal. A: Chem.* **2003**, *198*, 39−45.
(17) Ghosh, A. K.; Brindisi, M. Urea Derivatives in Modern Drug Discovery and Medicinal Chemistry. *J. Med. Chem.* **2020**, *63*, 2751−2788.
(18) Gallou, I.; Eriksson, M.; Zeng, X.; Senanayake, C.; Farina, V. Practical synthesis of unsymmetrical ureas from isopropenyl carbamates. *J. Org. Chem.* **2005**, *70*, 6960−6963.
(19) Liu, P.; Wang, Z. M.; Hu, X. M. Highly efficient synthesis of ureas and carbamates from amides by iodosylbenzene-induced Hofmann rearrangement. *Eur. J. Org. Chem.* **2012**, *2012*, 1994−2000.
(20) Spyropoulos, C.; Kokotos, C. G. One-pot synthesis of ureas from Boc-protected amines. *J. Org. Chem.* **2014**, *79*, 4477−4483.

https://doi.org/10.1021/acs.oprd.2c00229
Org. Process Res. Dev. 2022, 26, 3089−3095